

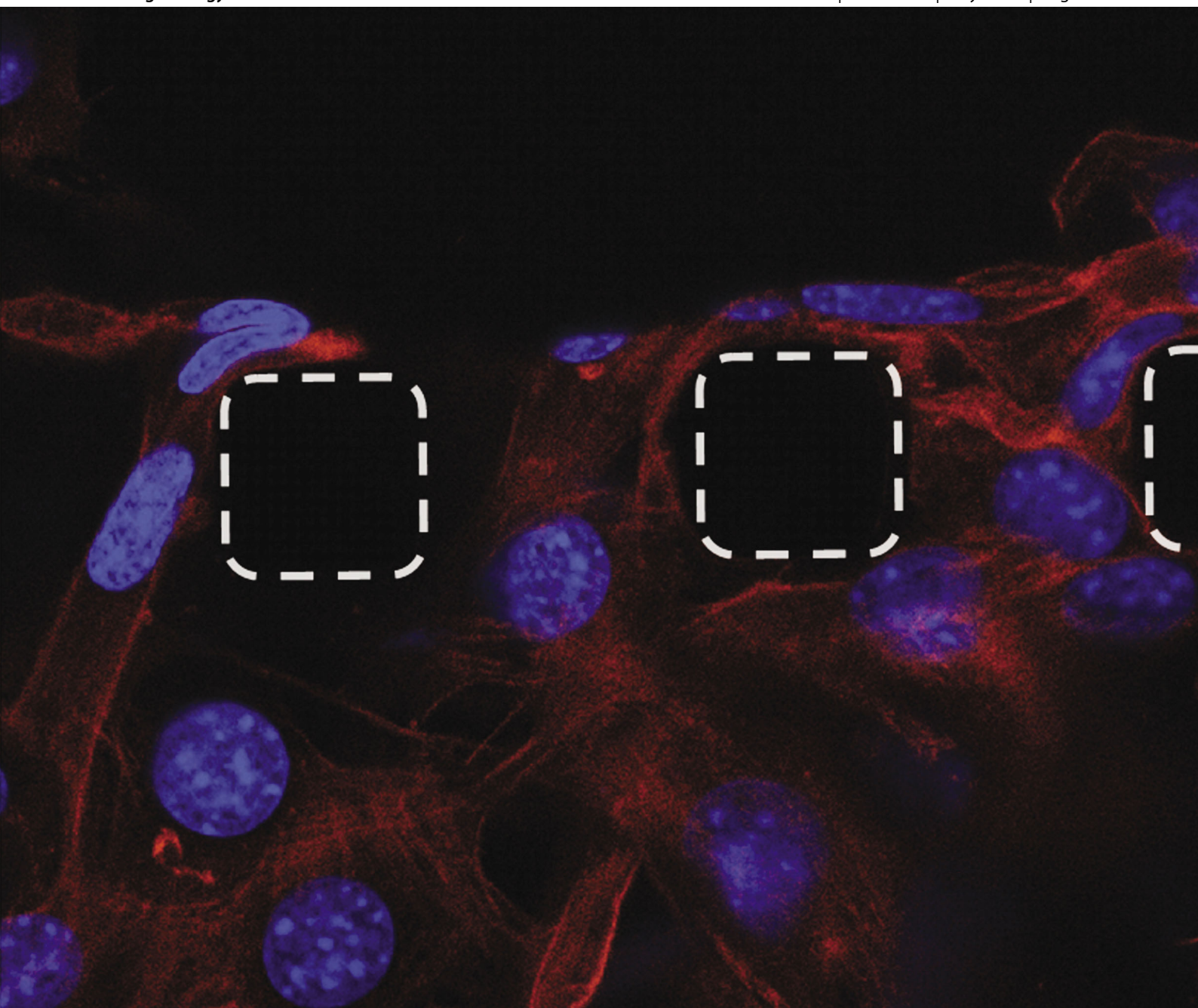
Indexed in
MEDLINE!

Integrative Biology

Quantitative biosciences from nano to macro

www.rsc.org/ibiology

Volume 3 | Number 7 | July 2011 | Pages 709–794



ISSN 1757-9694

RSC Publishing

PAPER

Ayala and Desai

Integrin $\alpha 3$ blockade enhances microtopographical down-regulation of α -smooth muscle actin: role of microtopography in ECM regulation



1757-9694(2011)3:7;1-Q

Cite this: *Integr. Biol.*, 2011, **3**, 733–741

www.rsc.org/ibiology

PAPER

Integrin $\alpha 3$ blockade enhances microtopographical down-regulation of α -smooth muscle actin: role of microtopography in ECM regulation†

Perla Ayala^a and Tejal A. Desai^{*ab}

Received 1st February 2011, Accepted 20th May 2011

DOI: 10.1039/c1ib00012h

Development of functional engineered matrices for regenerative therapies can benefit from an understanding of how physical cues at the microscale affect cell behavior. In this work, we use microfabricated systems to study how stiffness and microscale topographical cues in the form of “micropegs” affect extracellular matrix synthesis. Previous work from our lab has shown that microtopographical cues in 2D and 3D systems decrease cellular proliferation and regulate matrix synthesis. In this work, the combined role of stiffness and topography on ECM synthesis is investigated in a 2D micropeg system. These studies show that fibroblasts cultured on polydimethylsiloxane (PDMS) substrates with micropegs have reduced expression of collagen type I (Col I) and collagen type VI (Col VI) compared to fibroblasts cultured on flat substrates. In addition, cells on micropegged substrates exhibit down-regulation of other important regulators of ECM synthesis such as α -smooth muscle actin (α -SMA), and integrin $\alpha 3$ (Int $\alpha 3$). Interestingly, this effect is dependent on the contractility and adhesion of the cells. When cultured in the presence of RhoA kinase (ROCK) and myosin light chain kinase (MLCK) inhibitors, no significant differences in the expression of collagen, α -SMA, Int $\alpha 3$, and TGF β 1 are observed. Additionally, disruptions in cell adhesion prevent microtopographical regulation of ECM synthesis. When using an antibody to block the extracellular domain of Int $\alpha 3$, no differences in the expression of collagen are observed and blocking Int $\alpha 3$ results in enhanced down-regulation of α -SMA on the stiffer micropegged substrates. These findings demonstrate that regulation of extracellular matrix production by cells on a synthetic substrate can be guided *via* physical cues at the microscale, and add to the body of knowledge on the role of integrin-mediated mechanotransduction.

^a UCSF/UC Berkeley Joint Graduate Group in Bioengineering, USA^b Department of Physiology, Department of Bioengineering and Therapeutic Sciences, University of California, 203C Byers Hall Box 2520, 1700 4th Street, San Francisco, CA 94158-2330, USA. E-mail: tejal.desai@ucsf.edu; Fax: +1 415 514 4503; Tel: +1 415 514 4503

† Electronic supplementary information (ESI) available. See DOI: 10.1039/c1ib00012h

1. Introduction

The major objective in the development of engineered tissues is to design and create scaffolds that will properly integrate with the host tissue to support the regenerative process. *In vivo* the microenvironment provides cells with the necessary chemical signals to modulate cell migration, proliferation,

Insight, innovation, integration

Extracellular matrix remodeling plays a significant role in the regenerative process. In this study, synthetic scaffolds with 3D microfabricated projections are utilized to determine the role of stiffness and microscale topographical cues on cell–microenvironment interactions and ECM synthesis. Previous work showed that micropegged polydimethylsiloxane scaffolds reduced fibroblasts proliferation compared to flat substrates. Here, we show that stiffer microtopographical

cues can more effectively down-regulate gene expression of tissue fibrosis associated markers. This effect was found to be dependent on cell contractility and cell adhesion. Integrin $\alpha 3$ was found to be important in microtopographical regulation of α -smooth muscle actin expression. This work highlights the critical role of microscale physical cues in matrix remodeling and provides valuable knowledge for the development of superior regenerative therapies.

and differentiation. Likewise, biophysical signals and mechanical stresses from the extracellular matrix (ECM) can be converted into intracellular responses that regulate cell behavior and fate. The utilization of appropriate cues in tissue engineered platforms would ensure successful control of cellular behavior. Recent studies have highlighted the importance of physical properties on scaffolds where cells are guided towards the correct phenotype and suitable behavior. On rigid ECM scaffolds brain tumor cells spread, form stress fibers, and migrate rapidly. On softer ECM scaffolds with rigidity comparable with normal brain tissue, tumor cells appear rounded and fail to migrate.¹ Muscle stem cells cultured on hydrogel substrates that mimic the elasticity of muscle (12 kPa) self-renew *in vitro* and contribute to muscle regeneration when transplanted into mice.² Microfabricated topography in a PCL thin film enhanced the attachment and organization of retinal progenitor cells and induced cellular differentiation compared to flat thin films.³

An important challenge in tissue regeneration by exogenous cells, engineered scaffolds, or combinatorial therapy is the ability to create an *in vivo* environment that is receptive to treatment especially in aged, injured, and diseased tissues. The extracellular matrix in particular plays a critical role in cell behavior and *vice versa* the cell regulates the deposition of ECM molecules based on cues from this closed feedback loop. The ECM's inherent properties regulate several cellular functions including organization, proliferation, differentiation, and migration.⁴ In particular, studies have shown that the elasticity of the ECM can significantly affect cellular phenotype, migration and differentiation.⁵ An increase in tissue stiffness can be associated with the excess deposition of extracellular matrix proteins, a process known as fibrosis. This stiffening has been connected with pathological conditions including cancer and heart failure.⁶

The success of cardiac tissue regeneration approaches is highly dependent on the ability to generate an appropriate micro-environment that can restore myocardial function and support optimal healing, rather than over-expression of fibrous tissue. Major challenges for current approaches in stem cell regenerative therapy are cell survival and the formation of scar tissue that leads to differentiation of stem cells into unwanted phenotypes.⁷ Providing a scaffold that could facilitate cell retention and would allow for healing without fibrosis could alleviate these problems. Controlling fibroblasts, the main producers of collagen and other ECM molecules, is an important step to support the intrinsic regenerative process.

Effective manipulation of the cues that cells encounter in their microenvironment can greatly impact cell phenotype. It is now evident that mechanical, topographical, and geometrical cues can be utilized to modulate cellular morphology and behavior in 2D and 3D systems.^{5b,8} Previous studies have revealed that microtopographical cues can play a significant role in fibroblast proliferation. Neonatal rat ventricular fibroblasts (NRVF) showed decreased proliferation when cultured on 2D surfaces with micropegs compared to flat surfaces.^{8a} This observation was correlated with a significant decrease in cyclin D1 expression indicating that cell proliferation was affected at the level of G1/S cell cycle transition.^{8a} Furthermore, it was observed that when fibroblasts from the 3T3 cell line were cultured on the micropeg substrates, the decrease in proliferation was dependent

on local micropeg–cell interactions and was regulated by contractile mechanics.⁹ It was also shown that micropegs enhanced cell–scaffold adhesive interactions without changing the cell's elasticity. Additionally, adhesion to micropegs increased the expression of RhoA GTPase, myosin heavy chain II (MYH2), and connexin 43 (Cxn 43) in myoblasts.¹⁰

How the microenvironment can alter the remodeling of the ECM is not as well understood. Studies have also highlighted the impact mechanical stretch can have on fibroblast phenotype and ECM synthesis.¹¹ In particular, it has been observed that tissue stretch can decrease soluble transforming growth factor β 1 and procollagen type I in mouse subcutaneous connective tissue after injury.^{11a} Myofibroblast phenotype can be reversed to fibroblast phenotype with decrease in collagen production after mechanical stretch.^{11c} However, regulation of cell phenotype, gene expression, and ECM synthesis using microtopographical cues has not been fully explored. An understanding of how cell adhesion and interaction to micro-fabricated scaffolds affects cell behavior will supply critical information for the rational design of tissue engineering scaffolds.

In this work, we utilize micropegged silicone scaffolds to determine if regulation of ECM synthesis can be accomplished by using microscale topographical cues. In addition, we investigate the role of stiffness in microtopographical regulation of gene expression and ECM synthesis. Knowledge of the role of topography in matrix remodeling can be used to design and develop improved engineered regenerative therapies.

2. Results

Fibroblasts actively interact with the micropegs forming a three-dimensional network

In this work polydimethyl siloxane (PDMS) flat and micropegged scaffolds of different stiffness were created to determine if surface elasticity and microtopography can influence fibroblasts' production of extracellular matrix proteins. To prepare the substrates with different stiffness (1.79 MPa and 50 kPa) the elastomer to crosslinker ratio was varied based on a protocol by Brown *et al.*^{8b} Cells were seeded on PDMS substrates that had been oxygen plasma treated and incubated in media for at least 1 h. Fibroblasts were cultured for five days to allow for cells to proliferate and synthesize their own ECM. To observe the interaction of fibroblasts with the micropegged substrates a time lapse video was obtained after three days of culture. Cells attached to substrates and actively interacted with the micropegs, aligning with a set of micropegs, attaching to a micropeg, or releasing micropegs to bring other cells to attach to the micropegs (Fig. 1). After five days of culture, cells were fixed, stained, and imaged using confocal microscopy. Cells that maintained a close interaction with micropegs formed a three-dimensional network with the micropegged substrate. Cells preferentially attached to micropegs and interestingly also formed bridges across micropegs (Fig. 2). Cells attach and display similar cytoskeleton organization on both the 1.79 MPa and the 50 kPa substrates. Substrate elasticity did not affect cell morphology and cell interaction with micropegs as analyzed by image analysis of cell area and cell shape index (Fig. S1, ESI†).

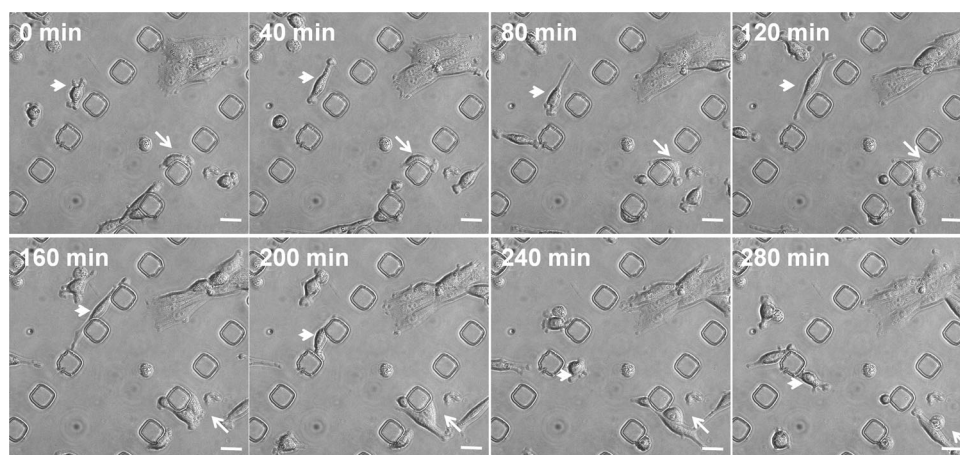


Fig. 1 Fibroblasts actively interact with the micropegs. Time lapse bright field imaging of fibroblasts at day 3 interacting with the micropegs. Short arrows follow cell number 1 and long arrows follow cell number 2. Cells actively attach, align, and detach from the micropegs to bring other cells in contact with micropegs. Scale bar, 25 μm .

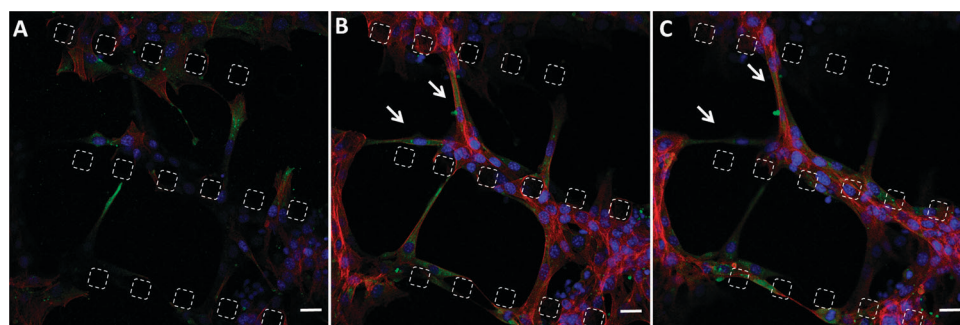


Fig. 2 Fibroblasts form a three-dimensional network with the micropegged substrate. Confocal imaging at day 5 reveals cells interacting with the micropegs at the (A) bottom, (B) middle, and (C) top of the micropegs (50 kPa substrate). Arrows show cells bridging micropegs. Blue: nuclei, red: F-actin, green: α -SMA. Scale bar, 25 μm .

Microtopography and stiffness influence collagen synthesis

To investigate how the mRNA expression of the extracellular matrix and other known fibrotic markers is affected by microtopography and stiffness, fibroblasts were cultured for five days on flat and micropegged substrates with elastic moduli of either 1.79 MPa or 50 kPa. Cells were lysed and mRNA content was analyzed by doing qPCR analysis. It was found that fibroblasts on substrates with micropegs have reduced expression of collagen type I (Col I), collagen type VI (Col VI), α -smooth muscle actin (α -SMA), and integrin α 3 (Int α 3) compared to fibroblasts cultures in flat substrates (Fig. 3A). No significant difference in mRNA expression of the genes investigated was observed between the cells cultured on the 1.79 MPa flat substrates and the cells cultured on the flat 50 kPa substrates. There was no statistically significant down-regulation on Col I and Int α 3 expression when cells were cultured on the softer micro-pegs (50 kPa). These markers were chosen to be analyzed since they have been shown to be elevated after myocardial infarction.¹² The results for transforming growth factor β 1 (TGF β 1) follow the same trend of mRNA expression on the different substrates.

These findings suggest that micropeg stiffness impacts expression of these genes but stiffness of a flat substrate in the range investigated does not have a significant impact.

Immunofluorescence staining and western blot analysis were done to qualitatively determine changes at the protein level. There was a decrease in the production of procollagen 1A (ProCol 1A) (Fig. 3B) and Col VI (Fig. S2A, ESI \dagger) on the micropegged substrates compared to the flat substrates which is consistent with our qPCR analysis. Additionally, there was reduced expression of α -SMA (Fig. 4B and Fig. S2B, ESI \dagger) and Int α 3 (Fig. 3C and Fig. S2C, ESI \dagger) in fibroblasts cultured on micropegged substrates compared to cells cultured on flat substrates.

Inhibition of cell contractility prevents micro-topographical regulation of gene expression

Fibroblasts were cultured on flat and micropegged PDMS substrates of different stiffness in the presence of pharmacological inhibitors for Rho kinase (ROCK) and myosin light chain kinase (MLCK) to determine how inhibiting cell contractility influences microtopographical regulation of mRNA expression. The fibroblasts' morphology was altered in the presence of both ROCK inhibitor (Y27632) and MLCK inhibitor (ML7). Cells cultured in the presence of ROCK inhibitor showed more elongated morphology and more cells were in contact with micropegs than in control (Fig. 4B and Fig. S3, ESI \dagger). Cells cultured in the presence of MLCK

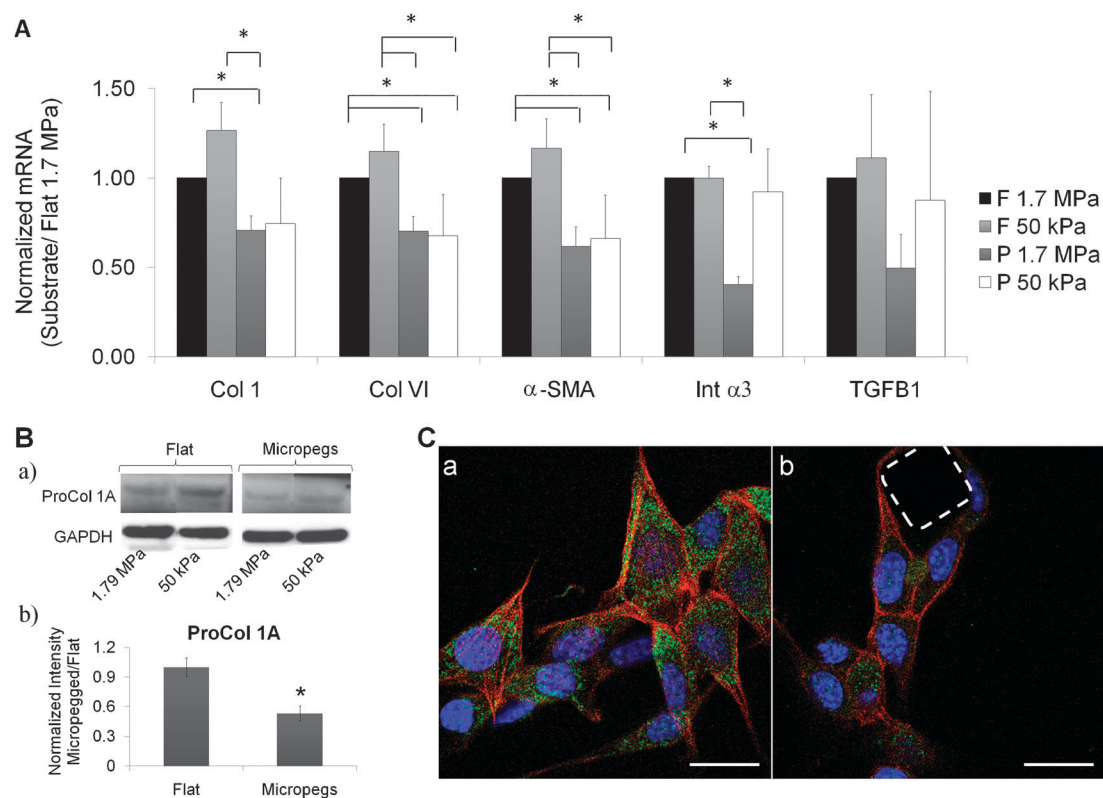


Fig. 3 Microtopography and stiffness influence gene expression and collagen synthesis. (A) Fibroblasts on substrates with micropegs (P) have reduced expression of collagen type I and collagen type VI, α -SMA, and integrin $\alpha 3$ compared to fibroblasts cultures in flat substrates (F) as analyzed by qPCR. Data are normalized to GAPDH and a 1.79 MPa flat substrate. Bars represent SEM and (*) indicates $p < 0.05$ ($n = 5$). (B) Fibroblasts on micropegged substrates have reduced procollagen 1A synthesis compared to cells on flat substrates as analyzed by (a) Western Blot and (b) immunofluorescence staining. (C) Immunofluorescence staining shows decreased integrin $\alpha 3$ expression in cells cultured on micropegged substrates (b) compared to cells cultured on flat substrates (a). Dashed line indicates micropeg. Blue: nuclei, red: F-actin, green: integrin $\alpha 3$. Scale bar, 25 μ m.

inhibitors showed slightly less elongation compared to ROCK inhibited cells (Fig. 4B and Fig. S3, ESI[†]). Microtopographical regulation of gene expression was dependent on the contractility of the cells. Analysis of mRNA expression by qPCR showed no significant difference in gene expression on micropegged surfaces compared to flat surfaces when cells were cultured in the presence of both ROCK inhibitor and MLCK inhibitor (Fig. 4A). Additionally, immunofluorescence staining showed no changes in α -SMA expression (Fig. 4B, Fig. S4A and S4B, ESI[†]) in fibroblasts cultured on micropegged substrates compared to cells cultured on flat substrates. In contrast with ROCK inhibited cells, fibroblasts grown in the presence of MLCK inhibitors showed mRNA expression patterns which follow studies in the absence of inhibitors.

Integrin $\alpha 3$ blockade enhances microtopographical down-regulation of α -smooth muscle actin and prevents regulation of collagen expression by microtopography

To determine if down-regulation of collagen and α -smooth muscle actin by microtopography was dependent on cell adhesion and integrin mediated mechanotransduction, cell cultures were treated with a functional antibody against the extracellular domain of integrin $\alpha 3$. With the antibody present, cells grown on micropegged substrates seem to recover the normal phenotype (Fig. S3, ESI[†]). Although cells cultured on

micropegs displayed restored morphology compared to cells on flat substrates, disruptions in cell adhesion prevented microtopographical regulation of ECM. Interestingly, when the extracellular domain of integrin $\alpha 3$ was blocked, enhanced down-regulation of α -SMA expression in cells cultured on the stiffer micropegged substrates was observed compared to cells cultured on the flat substrate, but no differences in the expression of Col I, Col VI, and TGFB1 were observed (Fig. 5A). Immunofluorescence staining showed reduced expression of α -SMA in fibroblasts cultured on micropegged substrates compared to cells cultured on flat substrates in the presence of the integrin $\alpha 3$ blocking antibody (Fig. 5B and Fig. S4C, ESI[†]).

3. Discussion

In this work we explored the incorporation of microtopographical cues in the form of micropegs on a 2D scaffold as a way to regulate expression of extracellular matrix molecules and other fibrotic markers. The critical role that fibroblasts have in myocardial remodeling has rendered them an attractive therapeutic target for the treatment of the failing heart and other fibrotic pathologies.¹³ Myofibroblasts, which are activated fibroblasts with the novo expression of α -smooth muscle actin (α -SMA),¹⁴ are found at the infarct site after day

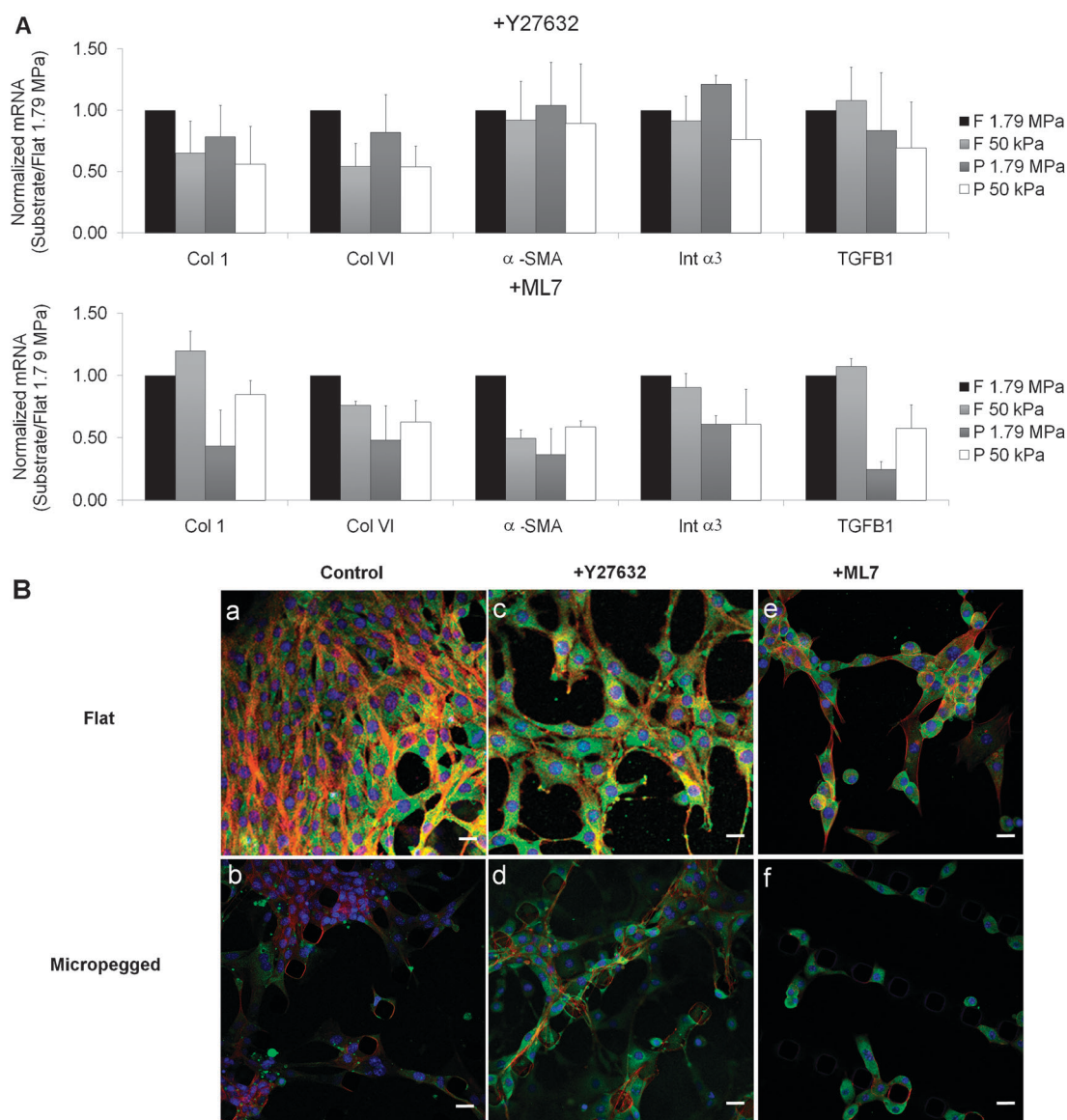


Fig. 4 Inhibition of cell contractility prevents microtopographical regulation of gene expression. (A) When cells are cultured in the presence of ROCK inhibitor (Y27632) no differences in the expression of collagen, α -SMA, Int α 3, and TGFB1 are observed among the different groups. In the presence of myosin light chain kinase inhibitor (ML7) microtopography regulation is attenuated but data did not reach statistical significance. Data are normalized to GAPDH and a 1.79 MPa flat substrate. Bars represent SEM ($n = 3$). (B) Immunofluorescence staining of α -SMA on flat (top) and micropegged (bottom) on 1.79 MPa substrates at day 5. (a, b) Control, (c, d) treated with ROCK inhibitor (Y27632), and (e, f) treated with MLCK inhibitor (ML7). Blue: nuclei, red: F-actin, green: α -SMA. Scale bar, 25 μ m.

3–4 post-infarction. Myofibroblasts are considered the main synthesizers of collagen and other ECM molecules after tissue injury, but in contrast with other tissues, cardiac myofibroblasts remain in the infarct site years after the myocardial infarction.¹⁵

Although there is a significant increase in collagen I, collagen III, and collagen VI production in cardiac pathology after myocardial infarction, recent studies have shown that collagen VI in particular plays an important role in myofibroblast expression, and the origin of fibrosis in the heart and in other diseased tissues as well.¹⁶ In this work, it was observed that fibroblasts' extracellular matrix synthesis is down-regulated by microtopography on two dimensional PDMS substrates. Micropegs also down-regulate the expression of α -smooth muscle actin, integrin α 3, and TGFB1, however, this effect

seems to be dependent on micropeg stiffness. When cells were cultured on the softer micropegs (50 kPa), there was no statistically significant down-regulation on Col I and Int α 3 expression. The expression of collagen type VI correlated with the expression of α -SMA which is in agreement with an earlier study which showed that collagen type VI induces the cardiac myofibroblast phenotype.^{16b}

Our previous studies have shown that micropegs reduced primary cardiac fibroblast proliferation,^{8a} and the interaction of 3T3 fibroblasts with the micropegs resulted in a decrease in BrdU incorporation compared to fibroblasts only contacting the flat areas of the substrate.⁹ Moreover, when cardiac myocytes were cultured on similar micropegged substrates they displayed *in vivo* like phenotype and had greater attachment

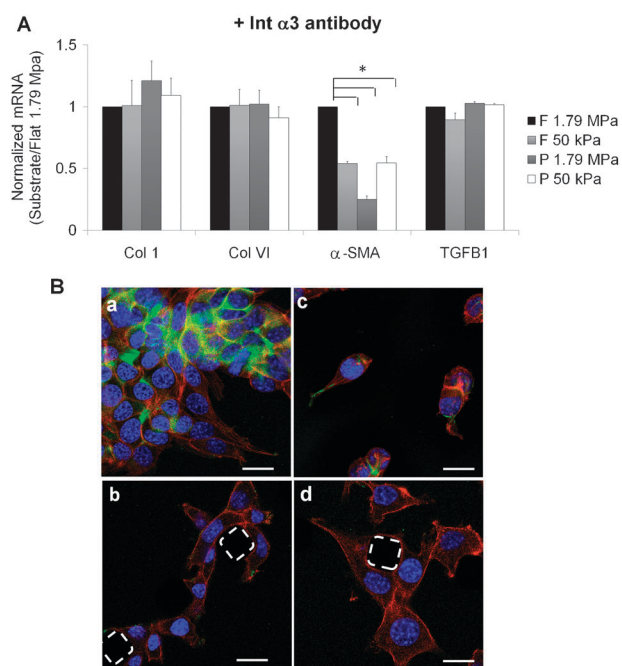


Fig. 5 Integrin $\alpha 3$ blockade enhances microtopographical down-regulation of α -smooth muscle actin and prevents regulation of collagen expression by microtopography. (A) When the adhesion molecule integrin $\alpha 3$ is blocked no differences in the expression of collagen type I, collagen type VI, and TGFB1 are observed. However blocking of integrin $\alpha 3$ enhances down-regulation of α -SMA on the micropegged substrates. Data are normalized to GAPDH and a 1.79 MPa flat substrate. Bars represent SEM and (*) indicates $p < 0.01$ ($n = 3$). (B) Immunofluorescence staining of α -SMA on flat (top) and micropegged (bottom) on 1.79 MPa substrates at day 3. (a, b) Control, and (c, d) treated with the integrin $\alpha 3$ antibody. Blue: nuclei, red: F-actin, green: α -SMA. Scale bar, 25 μ m.

and cell height compared to flat culture substrates.¹⁷ Surface topography also had a significant impact on gene expression and protein distribution which resulted in an increase in myofibrillar height and a decrease in cell area.¹⁸ Subsequently it was shown that microtopographical cues in a 3D system also inhibit fibroblast proliferation. SU-8 epoxy microrods suspended in matrigel significantly inhibited the proliferation of the fibroblasts as compared to a three-dimensional matrigel culture without microrods.^{8f} In contrast, these same microrods increased human mesenchymal stem cell proliferation and slowed osteogenic differentiation.¹⁹ Cardiac myocytes cultured in the presence of these microrods showed increased cross-sectional area and higher rates of spontaneous contraction.²⁰ In addition, it was observed that polyethylene glycol dimethacrylate (PEGDMA) microrods of different stiffness could affect proliferation and differentially regulate extracellular matrix production with stiffer microrods having a greater effect.²¹ Here we show that microtopographical cues on a two dimensional scaffold also down-regulate ECM synthesis and expression of fibrotic markers. Consistent with previous studies in a three dimensional system, stiffness of the microstructure is important in its ability to regulate gene expression.

These effects are dependent on the cell's ability to sense and interact with the microstructures through cell adhesion and

contractility. An important mediator of cytoskeletal tension is the small GTPase RhoA. It plays a critical role in the assembly of actin stress fibers in response to various stimuli such as cell adhesion, shape, and cytoskeletal tension.²² RhoA propagates downstream signals in effector proteins such as Rho associated Kinase (ROCK). Direct phosphorylation of the myosin light chain (MLC) by ROCK can lead to contractile force generation. Independent from RhoA, phosphorylation of MLC can also be regulated by Ca^{2+} -dependent myosin light chain kinase (MLCK). In this work, when the fibroblasts' myosin based-contraction was inhibited by two different independent mechanisms (ROCK and MLCK) there was no down-regulation of collagen synthesis and other fibrotic markers on micropegged substrates compared to flat substrates. These observations are consistent with previous studies in 2D micropegged surfaces where modulation of cell proliferation was found to be contractility-dependent⁹ and treatment with Y27632 and ML7 resulted in increased cell proliferation.²³ Inhibition of ROCK with Y27632 suppressed the micropegs' ability to regulate gene expression. Treating cells with ML7 resulted in attenuation of microtopographical regulation of mRNA expression since the mRNA expression trends remained similar to that of untreated cells. It was previously shown that cells on micropegged substrates displayed greater tether lengths compared to cells on flat substrates.¹⁰ This difference in tether length was also observed after treatment with ML7 and cells on micropegged substrates displayed similar tether lengths to cells cultured on untreated flat substrates suggesting that micropegs could rescue contractility. Treatment with Y27632 prevented differences in tether length between cells on flat substrates and cells on micropegged substrates.¹⁰ Taken together, these observations suggest that contractility inhibition with ML7 seems to only attenuate microtopographical regulation of cell proliferation and gene expression whereas inhibition with Y27632 results in suppression of microtopographical regulation. ML7 targets MLCK which only phosphorylates the myosin light chain, while Y27632 targets ROCK which phosphorylates MLC, inhibits myosin light chain phosphatase (MLCP) and can also activate LIM Kinase (LIMK) which regulates actin cytoskeletal organization.²⁴ Previous studies indicate that MLCK is responsible for MLC phosphorylation at the periphery and ROCK regulates MLC phosphorylation in the center of cells which results in decreased focal adhesion maturation in the center.²⁵ Cells cultured with ML7 have rescued contractility by ROCK activity in the center, and MLCK activity rescues contractility in the periphery when cells are treated with Y27632. This indicates that microtopographical regulation depends on cell contractile mechanics. Specifically, mechanotransduction signals might be more closely dependent on the formation of focal adhesions in the center of the cell than at the periphery.

In addition, it was observed that blocking the extracellular domain of integrin $\alpha 3$ hindered the micropegs' ability to down-regulate the expression of collagen, and enhanced the down-regulation of α -SMA by the micropegs. Integrins are the main receptors that form transmembrane connections between the extracellular matrix and the actin cytoskeleton. In the infarcted myocardium integrin $\alpha 3$ is elevated 3 days post-MI and precedes the expression of myofibroblasts and

collagen VI. It has been observed that both types collagen VI and collagen III interact with the integrin $\alpha 3$ receptor in cardiac fibroblasts.^{12a} In this work, fibroblasts cultured in the presence of the integrin $\alpha 3$ antibody displayed more rounded morphology and fewer cell to cell connections. These observations are consistent with earlier studies which showed that $\alpha 3\beta 1$ -deficient keratinocytes failed to polarize in the direction of the wound and instead scattered at random as individual cells rather than a cohesive monolayer.²⁶ In a different study it was observed that the inhibition of the integrin $\alpha 3$ extracellular domain resulted in reduced myoblast adhesion and decreased fusion index.²⁷ Moreover, studies have shown that blocking the functionality of the $\alpha 3$ integrin receptor with an antibody can lead to an attenuation of type VI collagen induced myofibroblast differentiation.^{12a} And recently a study also showed that deletion of integrin $\alpha 3$ prevented epithelial–mesenchymal transition, a source of myofibroblasts in lung fibrosis.²⁸ Thus, integrin $\alpha 3$ is implicated as an important regulator of cell phenotype, cell–cell interactions, and matrix deposition. Our studies indicate that expression of this molecule could be down-regulated by stiffer micropegs. Additionally blocking integrin $\alpha 3$ enhanced the down-regulation of α -smooth muscle actin by the microtopography, but disruption of cell adhesion abrogated regulation of ECM. These observations suggest that microtopographical regulation of ECM is cell adhesion dependent whereas α -SMA expression is closely regulated by integrin $\alpha 3$. Fibroblasts on micropegged substrates may have reduced integrin $\alpha 3$ expression even in the presence of the blocking antibody, which results in enhanced α -SMA down-regulation on these substrates. Future studies could focus on the temporal expression of these markers and the specific pathways involved in microtopographical regulation of gene expression. Although integrins are generally associated with mechanotransduction pathways it will also be important to explore the role of other transmembrane proteins such as syndecan-4²⁹ in mechanotransduction by stiffness and microtopography.

4. Conclusion

The present study demonstrates that microscale cues on a two dimensional scaffold affect gene expression, and extracellular matrix regulation. We utilized PDMS scaffolds of different stiffness with topographical cues in the form of micropegs to investigate the role of microtopographical cues in gene expression and extracellular matrix (ECM) synthesis. No differences in gene expression were observed on cells cultured on the flat substrates of different stiffness. Cells cultured on micropegged substrates showed reduced collagen synthesis and a decreased expression of other important markers elevated after myocardial infarction which are known to contribute to the remodeling process. Stiffer micropegged substrates had a greater effect than softer micropegged substrates. Moreover, microtopographical regulation of gene expression was found to be dependent on cell contractility and cell adhesion. When cells were cultured in the presence of contractility inhibitors, no significant differences in gene expression were observed. Functional blocking of Int $\alpha 3$ prevented regulation of ECM expression and enhanced microtopographical down-regulation of α -SMA. Overall, these

studies add to the body of knowledge showing the critical role physical cues alone have on cell behavior and performance. These findings highlight the influence of micro-scale cues on gene expression and the critical role of integrins in mechanotransduction. In addition, this knowledge could be applied towards the design of novel therapeutic platforms that could provide a microenvironment for optimal tissue regeneration.

5. Experimental section

Polydimethyl siloxane (PDMS) substrates

PDMS micropeg substrates were fabricated as reported previously.^{9,10} The micropegs are 15 μm tall with $25 \times 25 \mu\text{m}$ cross-sectional area, the spacing between micropegs is 125 μm from center to center of micropegs on one side and 50 μm spacing from center to center on the other side. To construct a photoresist mold, SU-8 2010 negative photoresist (Microchem, Newton, MA, USA) was spin-coated onto a single-crystal silicon wafer to a thickness of 15 μm and baked at 95 $^{\circ}\text{C}$ for 3 min. Microscale holes were introduced by placing a patterned photomask over the coated wafer and exposing it to UV light for 30 s at an intensity of 5 mW cm^{-2} . The uncrosslinked photoresist was then removed by washing the wafer in a SU-8 developer (Microchem, Newton, MA, USA) for 30 s, and then the SU-8 molds were baked at 95 $^{\circ}\text{C}$ for 3 min. The dimensions of the resulting microscale holes were then verified by light microscopy and surface profilometry. To create PDMS (Sylgard 184, Dow Corning, MI, USA) micropeg arrays with different elastic moduli (1.79 MPa and 0.05 MPa), the silicone elastomer base and the crosslinker were mixed thoroughly at different ratios (10:1 and 50:1, respectively) as previously reported.^{8b} The solution was degassed under vacuum, poured onto the SU-8 mold and spin-coated at 200 rpm for 1 min followed by 250 rpm for 30 s to achieve a thickness of 15 μm . The PDMS–wafer composite was then baked for 18 h at 60 $^{\circ}\text{C}$. After the PDMS was cured, the micropatterned PDMS membranes were peeled from the SU-8 masters. Unpatterned PDMS membranes were fabricated in an identical manner, except for the use of unpatterned, non-PR-coated silicon wafers as masters. Prior to use in cell culture experiments, the PDMS was rendered hydrophilic by exposure to oxygen plasma and then incubated with Dulbecco's Modified Eagle's Medium (DMEM) with 10% fetal bovine serum and 1% penicillin/streptomycin (Gibco-BRL, Grand Island, NY) for 1 h before seeding cells.

Cell culture

NIH 3T3 mouse fibroblasts were cultured in complete medium consisting of Dulbecco's Modified Eagle's Medium (DMEM) with 10% fetal bovine serum and 1% penicillin/streptomycin (Gibco-BRL, Grand Island, NY). Cell cultures were maintained in a humidity-controlled 5% CO_2 incubator at 37 $^{\circ}\text{C}$ and were allowed to grow to $\sim 90\%$ confluence. Prior to seeding, cells were trypsinized and resuspended in complete medium. Cells were plated at a density of 10 000 cells cm^{-2} and washed after 1 h to remove non-adherent cells.

Fluorescent microscopy

Cells were fixed in 4% paraformaldehyde (Fisher Scientific, Pittsburgh, PA) for 15 min, permeabilized with 0.5% Triton X-100 (Sigma, St. Louis, MO) for 15 min, and blocked with 1% bovine serum albumin (BSA) (Sigma, St. Louis, MO) for 30 min. F-Actin was stained using Alexa Fluor 563 phalloidin (Molecular Probes, Eugene, OR) for 30 min. To stain α -SMA, Int α 3, or procollagen 1A cells were incubated with mouse anti- α -SMA IgG (Sigma, St. Louis, MO), anti-Int α 3 IgG, (Santa Cruz Biotechnology, Santa Cruz, CA) and anti-ProCol 1A (Santa Cruz Biotechnology, Santa Cruz, CA), respectively, for 1.5 h at room temperature, and incubated with Alexa 488-conjugated donkey anti-mouse IgG (Molecular Probes, Eugene, OR, USA) for 1 h at room temperature. Nuclei were then stained with Hoechst 33258 (Molecular Probes, Eugene, OR, USA) for 5 min. Images were acquired using a Nikon TE2000E motorized inverted microscope or a Nikon C1si spectral confocal microscope. ImageJ was used to determine intensity levels of fluorescent images. Data are presented normalized to the flat substrate (1.79 MPa).

Quantitative PCR and mRNA expression

RNA levels were quantified after five days of culture using a Fast SYBR[®] Green Cells-to-CT[™] Kit (Applied Biosystems, Foster City, CA). Reverse transcription was performed on a Mastercycler S (Eppendorf, Hamburg, Germany). Quantitative PCR was performed using a StepOne Plus (Applied Biosystems, Foster City, CA). The primers used include: Col I forward primer 5'-GCACGAGTCACACCGGAAGT-3' and reverse 5'-AAGGGAGCCACATCGATGAT-3'; Col VI forward primer 5'-ACCCGGGACCGGCTACT-3' and reverse 5'-CAGAAGTCCATCCGTAATGAC-3'; α -SMA forward primer 5'-TCCTGACGCTGAAGTATCCGATA-3' and reverse 5'-GGTGCCAGATCTTTCCATGTC-3'; integrin α 3 forward primer 5'-ATCATCTCCTCTTGTGGAAGTG-3' and reverse 5'-GCCTTCTGCCTCTTAGCTTCATA-3'; GAPDH forward primer 5'-TGGCCTCCAAGGAGTAAGAAAC-3' and reverse 5'-GGGATAGGGCCTCTCTTGCT-3'; and TGF β 1 forward primer 5'-GAGGTCACCCGCGTGCTA-3' and reverse 5'-TGTGTGAGATGTCTTTGGTTTTCTC-3'. Each sample was analyzed in triplicate, and results were normalized to glyceraldehyde 3-phosphatedehydrogenase (GAPDH) and the flat PDMS substrates (1.7 MPa). Note that the lysate collected from micropegged scaffolds consists of mRNA from cells adhered to micropegs and cells adhered to the flat regions. Thus, comparative analysis results in a conservative underestimate of the effects of the micropegs on gene expression.

Western blotting

Protein levels were determined by Western blot, with detection by Horseradish peroxidase (HRP) conjugated secondary antibodies (Santa Cruz Biotechnology, Santa Cruz, CA) and development using a Novex ECL chemiluminescent substrate (Invitrogen). ImageJ was used to determine band intensity levels from the developed blots. All intensity levels were internally normalized to the loading control (GAPDH or α -tubulin) prior to calculating ratios of protein levels on

micropeg-textured *versus* flat scaffolds. Note that the lysate collected from micropegged scaffolds consists of protein from cells adhered to micropegs and cells adhered to the flat regions. Thus, comparative analysis results in a conservative underestimate of the effects of the micropegs on protein expression.

Time lapse imaging

To analyze the dynamics of fibroblasts interaction with the micropegs, cells were cultured on patterned PDMS substrates and allowed to grow for 3 days and then imaged for 15 h. Where indicated, the MLCK inhibitor ML-7, the ROCK inhibitor Y-27632 (Calbiochem, San Diego, CA), or the integrin α 3 antibody were diluted in complete medium prior to addition to cultures.

Contractility inhibition studies

To investigate the impact of cellular contractility, Y-27632 was used to inhibit Rho-associated kinase (ROCK) and ML-7 was used to inhibit myosin light chain kinase (MLCK) (Calbiochem, San Diego, CA, USA). Both drugs were diluted to 25 μ M in complete medium prior to addition to the cultures. In all cases, cells were seeded and allowed to attach and spread for 1 h before application of the drug, and the drug was left in the culture for 5 days prior to analysis.

Adhesion disruption studies

To investigate the impact of disruptions on cellular adhesion, cells were treated with a functional antibody against the extracellular domain of integrin α 3 (2 μ g mL⁻¹, Chemicon) in complete medium. In all cases, cells were seeded and allowed to attach and spread for 1 h before application of the antibody. Cells were cultured for 5 days prior to analysis.

Statistical analysis

A statistically significant difference among groups was detected by analysis of variance (ANOVA). Sequential Holm *t*-tests were then performed to identify differences between specific pairs of conditions.

Acknowledgements

We appreciate Dr Kurt Thorn's training and assistance at the Nikon Imaging Center at UCSF—Mission Bay. We also thank the UCSF Biomedical Micro- and Nanofabrication Core for allowing us to fabricate our Micropeg substrates. This research was partially supported by the National Science Foundation (NSEC), National Institutes of Health, a National Science Foundation Graduate Fellowship to P. A., and a University of California, Berkeley Chancellor's Fellowship to P. A.

References

- 1 T. A. Ulrich, E. M. de Juan Pardo and S. Kumar, *Cancer Res.*, 2009, **69**, 4167–4174.
- 2 P. M. Gilbert, K. L. Havenstrite, K. E. Magnusson, A. Sacco, N. A. Leonardi, P. Kraft, N. K. Nguyen, S. Thrun, M. P. Lutolf and H. M. Blau, *Science*, 2010, **329**, 1078–1081.
- 3 M. R. Steedman, S. L. Tao, H. Klassen and T. A. Desai, *Biomed. Microdevices*, 2010, **12**, 363–369.

- 4 (a) D. T. Butcher, T. Alliston and V. M. Weaver, *Nat. Rev. Cancer*, 2009, **9**, 108–122; (b) B. M. Gumbiner, *Cell (Cambridge, Mass.)*, 1996, **84**, 345–357; (c) C. M. Nelson and M. J. Bissell, *Annu. Rev. Cell Dev. Biol.*, 2006, **22**, 287–309; (d) E. W. Raines, *Int. J. Exp. Pathol.*, 2000, **81**, 173–182; (e) G. C. Reilly and A. J. Engler, *J. Biomech. Eng.*, 2009, **43**, 55–62.
- 5 (a) D. E. Discher, P. Janmey and Y. L. Wang, *Science*, 2005, **310**, 1139–1143; (b) A. J. Engler, S. Sen, H. L. Sweeney and D. E. Discher, *Cell (Cambridge, Mass.)*, 2006, **126**, 677–689; (c) D. S. Gray, J. Tien and C. S. Chen, *J. Biomed. Mater. Res., Part A*, 2003, **66**, 605–614.
- 6 (a) B. S. Bulew and K. T. Weber, *Herz/Kreislauf*, 2002, **27**, 92–98; (b) K. R. Levental, H. Yu, L. Kass, J. N. Lakins, M. Egeblad, J. T. Erler, S. F. Fong, K. Csiszar, A. Giaccia, W. Weninger, M. Yamauchi, D. L. Gasser and V. M. Weaver, *Cell (Cambridge, Mass.)*, 2009, **139**, 891–906.
- 7 M. Breitbach, T. Bostani, W. Roell, Y. Xia, O. Dewald, J. M. Nygren, J. W. Fries, K. Tiemann, H. Bohlen, J. Hescheler, A. Welz, W. Bloch, S. E. Jacobsen and B. K. Fleischmann, *Blood*, 2007, **110**, 1362–1369.
- 8 (a) S. Y. Boateng, T. J. Hartman, N. Ahluwalia, H. Vidula, T. A. Desai and B. Russell, *Am. J. Physiol. Cell Physiol.*, 2003, **285**, C171–C182; (b) X. Q. Brown, K. Ookawa and J. Y. Wong, *Biomaterials*, 2005, **26**, 3123–3129; (c) C. S. Chen, M. Mrksich, S. Huang, G. M. Whitesides and D. E. Ingber, *Science*, 1997, **276**, 1425–1428; (d) D. H. Kim, P. Kim, I. Song, J. M. Cha, S. H. Lee, B. Kim and K. Y. Suh, *Langmuir*, 2006, **22**, 5419–5426; (e) C. M. Nelson, R. P. Jean, J. L. Tan, W. F. Liu, N. J. Sniadecki, A. A. Spector and C. S. Chen, *Proc. Natl. Acad. Sci. U. S. A.*, 2005, **102**, 11594–11599; (f) J. J. Norman, J. M. Collins, S. Sharma, B. Russell and T. A. Desai, *Tissue Eng., Part A*, 2008, **14**, 379–390; (g) R. J. Pelham Jr. and Y. Wang, *Proc. Natl. Acad. Sci. U. S. A.*, 1997, **94**, 13661–13665; (h) S. R. Peyton, C. B. Raub, V. P. Keschrums and A. J. Putnam, *Biomaterials*, 2006, **27**, 4881–4893.
- 9 R. G. Thakar, M. G. Chown, A. Patel, L. Peng, S. Kumar and T. A. Desai, *Small*, 2008, **4**, 1416–1424.
- 10 A. A. Patel, R. G. Thakar, M. Chown, P. Ayala, T. A. Desai and S. Kumar, *Biomed. Microdevices*, 2010, **12**, 287–296.
- 11 (a) N. A. Bouffard, K. R. Cutroneo, G. J. Badger, S. L. White, T. R. Buttolph, H. P. Ehrlich, D. Stevens-Tuttle and H. M. Langevin, *J. Cell. Physiol.*, 2008, **214**, 389–395; (b) H. M. Langevin, N. A. Bouffard, G. J. Badger, J. C. Iatridis and A. K. Howe, *Am. J. Physiol.: Cell Physiol.*, 2005, **288**, C747–C756; (c) F. Poobalarahi, C. F. Baicu and A. D. Bradshaw, *Am. J. Physiol.: Heart Circ. Physiol.*, 2006, **291**, H2924–H2932; (d) J. Wang, A. Seth and C. A. McCulloch, *Am. J. Physiol. Heart Circ. Physiol.*, 2000, **279**, H2776–H2785.
- 12 (a) J. E. Bryant, P. E. Shamhart, D. J. Luther, E. R. Olson, J. C. Koshy, D. J. Costic, M. V. Mohile, M. Dockry, K. J. Doane and J. G. Meszaros, *J. Mol. Cell. Cardiol.*, 2009, **46**, 186–192; (b) P. E. Shamhart and J. G. Meszaros, *J. Mol. Cell. Cardiol.*, 2010, **48**, 530–537.
- 13 (a) P. Camelliti, T. K. Borg and P. Kohl, *Cardiovasc. Res.*, 2005, **65**, 40–51; (b) Z. Paz and Y. Shoenfeld, *Clin. Rev. Allergy Immunol.*, 2010, **38**, 276–286; (c) V. Polyakova, I. Loeffler, S. Hein, S. Miyagawa, I. Piotrowska, S. Dammer, J. Risteli, J. Schaper and S. Kostin, *Int. J. Cardiol.*, 2010.
- 14 B. Hinz, *J. Invest. Dermatol.*, 2007, **127**, 526–537.
- 15 (a) Y. Sun, M. F. Kiani, A. E. Postlethwaite and K. T. Weber, *Basic Res. Cardiol.*, 2002, **97**, 343–347; (b) Y. Sun and K. T. Weber, *Cardiovasc. Res.*, 2000, **46**, 250–256.
- 16 (a) P. Iyengar, V. Espina, T. W. Williams, Y. Lin, D. Berry, L. A. Jelicks, H. Lee, K. Temple, R. Graves, J. Pollard, N. Chopra, R. G. Russell, R. Sasisekharan, B. J. Trock, M. Lippman, V. S. Calvert, E. F. Petricoin, 3rd, L. Liotta, E. Dadachova, R. G. Pestell, M. P. Lisanti, P. Bonaldo and P. E. Scherer, *J. Clin. Invest.*, 2005, **115**, 1163–1176; (b) J. E. Naugle, E. R. Olson, X. Zhang, S. E. Mase, C. F. Pilati, M. B. Maron, H. G. Folkesson, W. I. Horne, K. J. Doane and J. G. Meszaros, *Am. J. Physiol.: Heart Circ. Physiol.*, 2006, **290**, H323–H330; (c) C. A. Sherman-Baust, A. T. Weeraratna, L. B. Rangel, E. S. Pizer, K. R. Cho, D. R. Schwartz, T. Shock and P. J. Morin, *Cancer Cell*, 2003, **3**, 377–386; (d) H. Mollnau, B. Munkel and J. Schaper, *Herz/Kreislauf*, 1995, **20**, 89–94.
- 17 J. Deutsch, D. Motlagh, B. Russell and T. A. Desai, *J. Biomed. Mater. Res.*, 2000, **53**, 267–275.
- 18 D. Motlagh, S. Senyo, T. A. Desai and B. Russell, *J. Mol. Cell. Cardiol.*, 2002, **34**, A32.
- 19 J. M. Collins, P. Ayala, T. A. Desai and B. Russell, *Small*, 2010, **6**, 355–360.
- 20 M. W. Curtis, S. Sharma, T. A. Desai and B. Russell, *Biomed. Microdevices*, 2010, **12**, 1073–1085.
- 21 P. Ayala, J. I. Lopez and T. A. Desai, *Tissue Eng. A*, 2010, **16**, 2519–2527.
- 22 K. Bhadriraju, M. Yang, S. Alom Ruiz, D. Pirone, J. Tan and C. S. Chen, *Exp. Cell Res.*, 2007, **313**, 3616–3623.
- 23 J. K. Biehl, S. Yamanaka, T. A. Desai, K. R. Boheler and B. Russell, *Dev. Dyn.*, 2009, **238**, 1964–1973.
- 24 K. Riento and A. J. Ridley, *Nat. Rev. Mol. Cell Biol.*, 2003, **4**, 446–456.
- 25 G. Totsukawa, Y. Wu, Y. Sasaki, D. J. Hartshorne, Y. Yamakita, S. Yamashiro and F. Matsumura, *J. Cell Biol.*, 2004, **164**, 427–439.
- 26 D. P. Choma, K. Pumiglia and C. M. DiPersio, *J. Cell Sci.*, 2004, **117**, 3947–3959.
- 27 E. Brzoska, V. Bello, T. Darrivere and J. Moraczewski, *Differentiation (Oxford, U. K.)*, 2006, **74**, 105–118.
- 28 Z. Borok, *J. Clin. Invest.*, 2009, **119**, 7–10.
- 29 R. M. Bellin, J. D. Kubicek, M. J. Frigault, A. J. Kamien, R. L. Steward, Jr., H. M. Barnes, M. B. DiGiacomo, L. J. Duncan, C. K. Edgerly, E. M. Morse, C. Y. Park, J. J. Fredberg, C. M. Cheng and P. R. LeDuc, *Proc. Natl. Acad. Sci. U. S. A.*, 2009, **106**, 22102–22107.